

Improving Interlocking Joint Robustness with Gradient-Descent Based Stiffness Optimization

Javier Linero-Quintana
Adviser: Ryan Adams

Abstract

This paper discusses the design, development, and evaluation of a finite-element analysis approach to optimizing the stiffness of interlocking joints used in manufacturing that revolves around woodworking. This project adapts a gradient-based optimization technique on a finite-element simulation software, to evaluate various joints, including dovetail, scarf, lap, gooseneck, rabbet, and a combination that exhibits complex joinery. The methodological approach involves an alternating penalty structure and randomization to simulate the deformation of these joints to optimize their parameters to minimize the displacement and maximize the stiffness while addressing the issue of local minima in gradient descent. While the tool maximizes the stiffness, we focus on minimizing the environmental impact by reducing the need for adhesives and mechanical fasteners. This research aims to extend previous work on traditional dovetail optimization techniques by providing a methodological approach that enables the adaptability of these tools to various piece-wise linear joints that can be used in complex joinery techniques. Thus we facilitate the ease of manufacturing and reassembly while providing insights that benefit our environmental sustainability.

1. Introduction

The disassembly of various objects including furniture, 3D printing, turbines, and other various industrial machinery, has become a crucial process in manufacturing. This practice is often required to address several constraints such as machine size limitations, shipping costs, and handling that many companies have to confront. Although this benefits manufacturers, it also simplifies the reassembly and maintenance of products for consumers. Nevertheless, ensuring that these reassembled products maintain structural integrity remains as a significant concern. To address

this, interlocking joints have offered robust and reliable connections that not only support structural demands but also enhance the durability of these objects.

Several advancements have leveraged machine learning techniques, including gradient descent and surrogate models, to optimize the design of the dovetail joints concerning stiffness [9], [3]. Although these advancements have played a crucial role in the improvement of dovetail joints, this process is even more invaluable for weaker joints such as scarf and lap joints, who inherent lower mechanical strengths due to their geometries. Such joints rely on adhesives, metal fasteners, or dowels to maintain structural integrity and are often presented in millwork. Although these fastening methods provide a temporary fix, they introduce vulnerabilities in terms of durability due to the differences in the material properties. This has become evident when showing respective responses to several environmental factors such as changes in temperature, humidity and corrosion, where it comprises the interlocking mechanism by deforming over time [6]. Not only does this deter the joint's effectiveness but it also increases the maintenance requirements that consumers have to face.



Figure 1: Designed wooden chair with disassembled components with interlocking joints [4]

Furthermore, improving the stiffness of the joints can significantly reduce the reliance on several fastening methods. This promotes the use of complex joinery that provides more sustainable, recyclable products that also provide cost-effective measures for manufacturers. For instance,

in traditional Japanese joinery, known as Sashimono, there have been adaptions of joints into complex designs that have been developed to ensure enhanced structural integrity with ease of assembly. As evidenced in figure 1, these adaptations have enabled the process of making furniture without adhesives and mechanical fasteners while maintaining its strength. In like manner, Jaewan Park, a conventional designer integrated gooseneck joints to produce reusable pencils that offer durable and environment-friendly solutions [5]. Numerous adaptions prioritize environmental sustainability which in turn reduces manufacturing costs, increasing consumer convenience, and thus underscoring the significant role of evaluating various optimized interlocking joints in the evolution of manufacturing practices.

Moreover, aforementioned research has concentrated on optimizing the design of dovetail joints, a traditionally strong joint that lacks diversification. There has been a significant research gap in the empirical evaluation and optimization of other common joints, such as scarf, lap, and gooseneck joints. This paper introduces a meticulous design and development approach to the optimization of stiffness in various locking joints. Using finite-element simulation software, we adopt a gradient-based optimization technique that allows for the assessment and refinement of these joint configurations. The approach enables the alternating penalty structure provided, which constricts one side of the interlocking joint at a time, allowing us to simulate the deformation of the joints under a fixed load [9]. This provides the optimization of the vectored shape parameters given a constrained partial differential equation, where we can apply the gradient descent to minimize the displacement of the interlocking joint and inherently maximize the stiffness. Ultimately, the goal of this project extends beyond solely maximizing the stiffness and shape design; it aims to enhance the application of diverse interlocking joints in complex joinery techniques to promote sustainability in our environment and cost-effectiveness for manufacturers and consumers.

The project implementation involved configuring shape parameters and creating triangular meshes for the finite-element simulation. Parameters were optimized to minimize the displacement under a fixed load, followed by modeling with CAD software for 3D printing. This setup required meticulous handling in hyperparameters and initialization of inputs to provide a robust procedure

that can generate optimal solutions.

Furthermore, our initial results indicate improvements in joint stiffness particularly for the lap and rabbet joints, which showed a significant increase in stiffness across two load intervals. There was also variability in performance due to limitations in the joint design's hyperparameter selection and printing quality. However, the overall results provide a strong basis for utilizing this technique to expand the space of sustainable complex joinery while providing robust connections.

2. Background and Related Work

Over the recent years, several implementations have been curated to inhibit the optimization of joint design with machine learning techniques. Xingyuan Sun explores the use of gradient-based methods for dovetail-joint shape optimization. Sun's work emphasizes on modeling the physical process of an interlocking joint deforming given an applied load to utilize a numerical method called the finite element method to analyze the system as a partial differential equation (PDE). Finite element analysis allows for the application of gradient-descent to minimize objective functions given their constraints. Enabling a differentiable simulator to model the contact and deformation between joint parts, allows for the use of machine learning techniques to optimize the parameters of a given shape. This paper uses an alternating penalty structure to accurately evaluate the displacement field of a given shape by keeping one side rigid at a time while the other deforms and labels the left and right bodies as Ω_L and Ω_R . The deformation of these bodies is formulated as:

$$\nabla \cdot \sigma = f \quad (1.1)$$

$$\sigma = \lambda \text{tr}(\varepsilon) I + 2\mu \varepsilon \quad (1.2)$$

$$\varepsilon = \frac{1}{2} (\nabla \mathbf{u} + (\nabla \mathbf{u})^T) \quad (1.3)$$

The given equilibrium formula 1.1 is broken down where $f = 0$ is the force that acts throughout the volume of the joint (i.e. gravity), where the stress tensor σ refers to the force applied to a material per unit area. In continuum mechanics, the stress tensor is characterized by Lamé parameters, λ , and

μ , which describe the material's response to deformation forces. These parameters are derived from the material's elasticity characters, specifically Young's modulus E and Poisson's ratio ν , which quantify the material's stiffness and its tendency to expand/contract in response to stress. These parameters are significant in modeling the physics of this system, and the calculations are discussed within the paper's implementation [9]. Likewise, there is a significant relationship between the stress and strain ε of an object, where the strain is the change in the shape that results from the applied force. This breaks down the stress tensor into 1.2, where $\text{tr}(\varepsilon)$ refers to the trace of the matrix, and I is the identity matrix. Furthermore, our strain vector ε is derived from 1.3, where it is calculated from a displacement vector \mathbf{u} . This formulation allows the application to use meshes in a differentiable simulator, enabling the optimization of an objective function within continuum mechanics.

$$\Pi_L := \int_{\Omega_L} \frac{1}{2} \varepsilon : \sigma dA - \int_{\Omega_L} f \cdot \mathbf{u} dA - \int_{\partial \Omega_L} T \cdot \mathbf{u} dx + w_{\text{pen}} \int_{\partial \Omega_L} \text{softplus}^2(-\text{sdf}(\mathbf{u}; \Omega_L, \Omega_R)) dx \quad (1.4)$$

Furthermore, the preceding formula provides the total potential energy of the system to a fixed traction force T and has a penalty regularizer that calculates the signed difference in terms of the displacement vector of the two bodies where the left body is fixed. This alternates between the bodies and promotes compliance with the fixed traction force while discouraging any significant discrepancies in the displacement vectors to have an accurate representation of the deformation. The shape design parameters are expressed as θ , where a displacement field $\mathbf{u}(\theta)$ allows for a calculation on the difference of average displacement in the horizontal direction between the left and right edges of a joint denoted as $d(\mathbf{u}(\theta))$. This allows for the construction of a final optimization objective function $L(\theta)$ that can apply the adjoint method, a computational method that formulates the gradients of an objective function to their respective parameters θ shown below.

$$L(\theta) := d(\mathbf{u}(\theta)) + w_{\text{min_l}} \cdot L_{\text{min_l}}(\theta) + w_{\text{min_w}} \cdot L_{\text{min_w}}(\theta) \quad (1.5)$$

Notably, this loss function contains two regularizers that conform to the relative design space of the

dovetail joints provided in the paper. These prevent the designated contact lengths and width of the joints from falling too short and will be discussed further in subsection 4.2. Ultimately this provides for a differentiable objective function that can be calculated as $\frac{dL(\theta)}{d\theta} = -\frac{\partial L(\theta)}{\partial \mathbf{u}} \left(\frac{\partial F}{\partial \mathbf{u}} \right)^{-1} \frac{\partial F}{\partial \theta} + \frac{\partial L(\theta)}{\partial \theta}$, where $F(\mathbf{u}, \theta) = 0$, is the provided PDE from the simulator. This ultimately minimizes the displacement of the two sides in a joint when applying a load, thus maximizing the overall stiffness and providing robust dovetail joint connections.

Analogously, there have been other implementations of improving dovetail joint design parameters using gradient-free optimization techniques, but require other systems like surrogate models to approximate improvements. For instance, Hahn and Cofer, implemented a surrogate model with a gradient-free optimizer for refining design parameters in complex dovetail joint designs to enhance a structural interlocking mechanism for turbines [3]. Through a finite element simulation tool, Abaqus, they've used the cross-section of their three-dimensional model to visualize the parameters required for optimization tools. The given surrogate models were made to approximate the given load on the dovetail joint to sample and optimize for their dovetail parameters. This approach provides a robust framework for fine-tuning joint designs under realistic loading conditions, however requires more computationally intensive methods to approximate a given model.

Subsequently, Sun's approach benefits significantly from the efficiencies offered by gradient-based optimization methods. Dokken et al. emphasize that these methods not only converge quickly but also maintain their efficiency regardless of how large the number of parameters are involved [1]. However, these papers primarily concentrate on optimizing traditional dovetail joints, which are already known for their inherent strength and efficiency in woodworking and manufacturing spaces. While the research makes significant strides in enhancing these joints through this optimization technique, they lack in diversification of other joint configurations that could be equally or more beneficial in various manufacturing scenarios. For example, the exploration of improved joint configurations could be introduced into making complex joinery that would lead to more sustainable approaches like Sashimono, that reduce the need for external materials such as adhesives and metal fasteners while providing robust connections.

3. Approach

This research aims to expand the application of optimization on dovetail joints utilizing the FEM, and a gradient-based optimization technique with the python package FEniCS,¹ to various interlocking joint types such as scarf, lap, and rabbet joints, which are typically more vulnerable and less studied. Extending previous research techniques to these joints, we seek to enhance their robustness and reduce the reliance on adhesives and metal fasteners as shown with complex joinery techniques. This approach not only extends Sun's paper in terms of an empirical evaluation but also provides a detailed methodology adaptable to various piecewise linear joint configurations, while also addressing issues with the optimization technique.

To further advance the gradient-based optimization, we introduce a randomized initialization step. Although the previous implementation provides a randomized walk to look for steeper gradients, the domain within a respective starting space is nevertheless relatively restricted. Therefore we introduce a randomized initialization step based on using the central limit theorem to provide variability in the starting angles across the interlocking joints. Starting from multiple randomly determined points in the solution space, the gradient-descent has a higher chance of discovering more globally optimal solutions rather than being confined to these local minimums.

This research departs from the traditional top-down symmetrical approach used in this particular implementation. Instead, we use a more flexible strategy that can be adapted to a variety of joint types. Likewise, we offer insights into the basic selection of hyperparameters to get any joint configuration to converge properly. This tailored optimization process, while accommodating the specific needs and constraints of different joint designs provides a general methodological approach to evaluate across any piece-wise linear joint. These optimized joints are then rigorously tested using an Instron machine, which allows for the precise control of applying fixed loads and giving accurate measurements of their performance relative to stiffness measured in load force per mm (F/mm). Through these tests, our research not only validates the theoretical models provided in

¹<https://fenicsproject.org/>

Sun’s implementation but also extends these techniques to broaden the manufacturing space to provide more reliable and effective solutions.

4. Implementation

This section will provide a simple iteration of the overall process required to achieve the goal of the project before running it through evaluation metrics. In terms of designs, we will have to begin by limiting the types of designs that allow for a machine direction tensile test; a method used to evaluate material properties such as tensile stress, strain, and displacement in a lengthwise direction as shown in figure 2. This results in an interlocking joint design, that has to be curated into shape parameters $\mathbf{x} \in \mathbb{R}^d$ where d is denoted as degrees of freedom (DoF). These parameters are configured into triangular meshes to use in the finite-element simulation, where the gradient-descent can be applied to solve the optimization function in formula 1.5. In light of this, we address the local minima issue while providing a randomized initialization method that curates numerous joint parameters/meshes that vary in shape angles. Furthermore, we apply the optimization technique to output optimized parameters $\mathbf{o} \in \mathbb{R}^d$ to minimize displacement. Ultimately, we choose the best-optimized version(s) and model them with computer-assisted design (CAD) software to 3D print the models for evaluation.

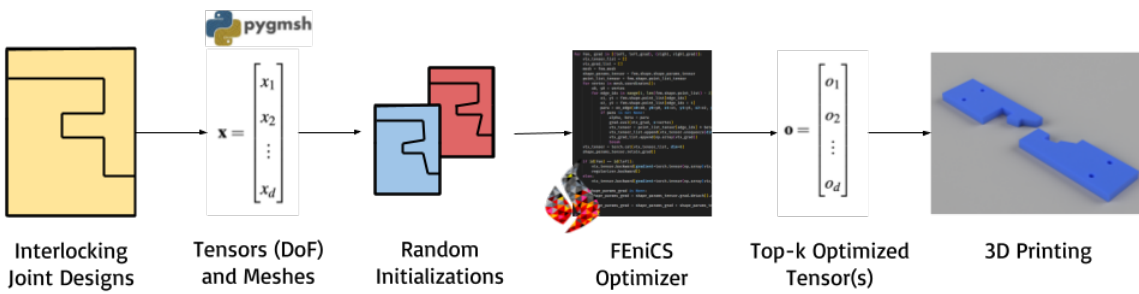


Figure 2: General overview of the implementation model.

4.1. Design Space

Provided that the goal of the project is to improve the stiffness of interlocking joints, tensile tests are vital in calculating the deformation in terms of stress, strain, and displacement allowing for the

optimization of shape design. The tests can either be performed in a machine or transverse direction, where the machine direction regards pulling the joints in the lengthwise direction whereas the other is set to be perpendicular from this typical form. Given that the previous implementation of the finite-element simulation tool was focused on dovetail optimization, it constricts to the machine direction and thus our design space similarly. Therefore to create an empirical evaluation, we choose 5 different interlocking joints that follow these constraints, and add the simple dovetail as a baseline model to validate the new implementation. These configurations shown in figure 3 include gooseneck, scarf, modified lap and rabbet joints, and a combination of dovetail/scarf to exhibit the future adaptions that can be made with complex joinery.

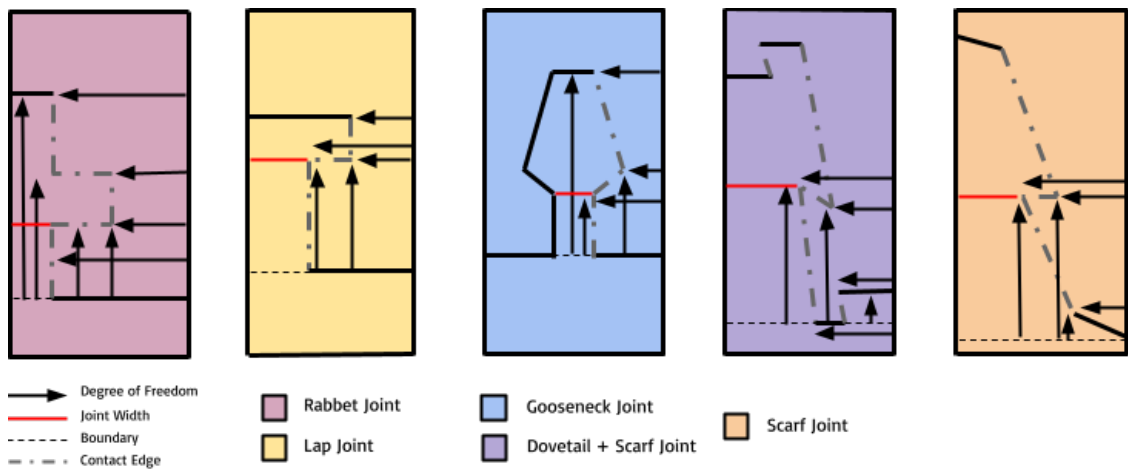


Figure 3: Joint Design with respective Parameters

Furthermore, there is a translation required to allow the finite-element simulation tool to evaluate the PDE in terms of parameters and calculate the stress and strain vectors needed to minimize the optimization function. To translate these interlocking joints, we utilize degrees of freedom to curate a tensor in PyTorch² expressed as \mathbf{x} [9]. The degrees of freedom as presented as one-dimensional vectors that are either in the horizontal or vertical dimensions and are combined to form the edges of a joint. They begin at a boundary wall shown in figure 3 to constrict the optimization in terms of the magnitude of the parameters and to focus on the geometries rather than a provided clamp space.

²<https://pytorch.org/>

Likewise, for the regularizers, we must label contact edges and joint widths to prevent the optimizer from making these parameters too small.

To finalize the translation for the tool, we utilize pygmsh³ to create triangular meshes from the parameters. Sun's implementation uses a top-down symmetrical approach to halve the computational resources needed for dovetail optimization. However, not all of the configurations in this new design space are symmetrical, thus requiring either setting a new domain for the optimization technique or temporarily halving the size parameters to fit within the boundaries and then sizing it up. The sub-package of the simulation tool, DOLFIN,⁴ requires to set this domain restriction with a Dirichlet boundary condition, which sets the specific values of a given boundary to solve the PDE. Although unsuccessful, we used the second option where the height was set to 12.5mm and scaled up as it provided closely accurate calculations. After examining these conditions, the shapes were modeled by constructing a dataset of parameters for each joint, and then a vectored mesh was created for the simulation as shown in figure 4.

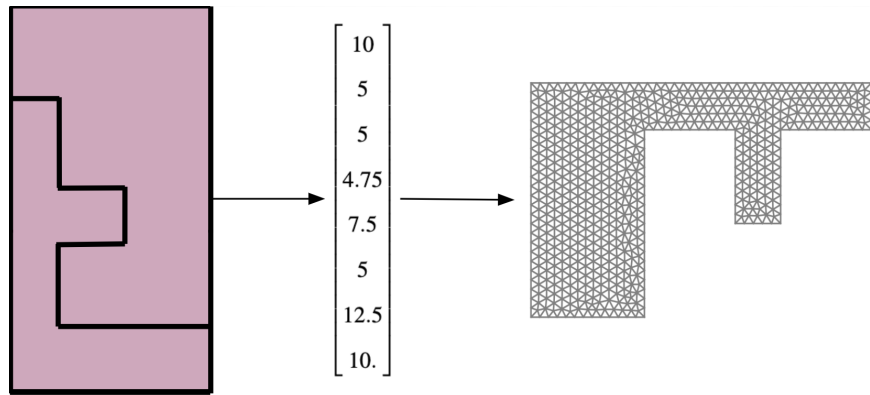


Figure 4: General overview of creating a joint's vectored mesh. Where we begin with a concept, break it up into degrees of freedom and use pygmsh to form the mesh.

4.2. Hyperparameters

Hyperparameters are essential in guiding the process of our constrained optimization problem. This section will provide an in-depth methodology for carefully selecting these to ensure the effectiveness of the optimization while adhering to these constraints. For a fixed traction force, we've noted this

³<https://pypi.org/project/pygmsh/>

⁴<https://fenicsproject.org/olddocs/dolfin/2019.1.0/python/>

parameter on the deformation of these joints is an integral component for the realistic approach the finite element method proposes. This is critically examined to strike a balance between the convergence and accuracy of a model’s deformation. The set traction force can’t be too small as it’ll cause the algorithm to take an impractically long time to converge, and likewise, it should not be too high as it’ll lead to infeasible optimization paths. After curating the shapes, we’ve processed several optimization attempts with different traction forces to obtain convergence and a feasible optimization time of around 4 to 5 minutes per initialization iteration, shown in table 1.

Next, our penalizing constraints are encapsulated in our model through the incorporation of regularizers of the shape parameters. These conform to two properties of the joints, their width and the length of the contact edges between the two bodies. The minimum contact length regularizer addresses joints to have sufficient contact area for joint integrity. The previous implementation sets the regularizer as $\max(\min_len - |l|, 0)^2$, where if the length is too small the regularizer will penalize by adding the squared difference with \min_len where it has been set to 1.5mm. Given that there are several contact edges in a configuration, this regularizer sums every contact edge labeled in the model to penalize. Similarly, the minimum width regularizer prevents the joint from having a narrow neck to ensure that the joint remains robust enough to handle the stresses of real-world applications. This regularizer follows a similar regularizer, $\max(\min_width - \text{width}(\theta), 0)^2$, where the $\text{width}(\theta)$ is calculated from the joint designs shown in 3 and the predetermined hyperparameter $\min_len = 2.5\text{mm}$.

| Joint Type | Degrees of Freedom | Traction Force (N) | Min Joint Width (mm) | Min Contact Length (mm) |
|----------------|--------------------|--------------------|----------------------|-------------------------|
| Simple | 3 | 0.001 | 2.5 | 1.5 |
| Rabbet | 7 | 0.001 | 3.5 | 2.5 |
| Gooseneck | 6 | 0.001 | 2.5 | 2.5 |
| Scarf | 6 | 0.003 | 3.5 | 2.5 |
| Lap | 6 | 0.003 | 3.5 | 2.5 |
| Dovetail Scarf | 8 | 0.010 | 3.5 | 2.5 |

Table 1: Optimization parameters for various joint types.

We note that these parameters penalize in a quadratic scale, that varying joint configurations differ when it comes to contact length and joint width and have to be hyper-parameterized to conform their spaces. Across the board, these joints had larger contact spaces requiring the change up to 2.5mm. Likewise, because rabbet and lap joints were on the edge of the joint rather than being centered as the dovetail and gooseneck, they required a 3.5mm minimum for their joint width. The two scarf joint widths are measured at the center point, resulting in larger widths which were settled at 3.5mm. The parameters for the dovetail joints in the dovetail scarf joint weren't changed as they were on the edges. After some considerable evaluation of each joint design, the following changes have been applied and shown in table 1.

4.3. Randomized Initialization

Gradient descent is a useful optimization algorithm that works in line with the parameters of an objective function to find minimums. However, a significant challenge associated with gradient descent is its tendency to converge to local minima, and this has led to the development of various strategies to tackle this. In the previous implementation, there is an adapted gradient descent algorithm that incorporates a "random walk" strategy [9]. This takes steps in a randomized direction to explore broader solutions that can help escape these local minimums. To further enhance the solution space the objective function provides, we implement randomized initialization to explore the wide range of angles that a joint's configuration can have.

To implement this feature effectively, our approach leverages the Central Limit Theorem (CLT) to approximate tensors and introduce variability in the shape angles of joints. This process begins by establishing the center shape parameter in a vertical position, as illustrated in figure 5. We conduct this to provide a consistent reference point where the adjustments and variability can be measured and evaluated systematically. We then initialize this method by creating a normal distribution of size 1000, with a mean equal to the magnitude of the degree of freedom in a given joint tensor ($\mu = |x_i|, \forall i \in d$), and a standard deviation of $\sigma = 0.5$ mm. This distribution provides a space from which we can sample randomly and effectively fulfill the theorem to approximate the population

mean. To approximate the population mean, we average these samples and create a degree of freedom that is relatively close, and given that we conform the center interlocking part of the joint to a vertical position, it allows for a controlled variability that sways the angle of the shape. The specified deviation not only changes the angles, but it produces slight variations in the magnitudes of all parameters and thus creates diverse joint configurations to enhance the optimization's process in escaping local minima. This iterative process is repeated 20 times to ensure a diverse selection of configurations.

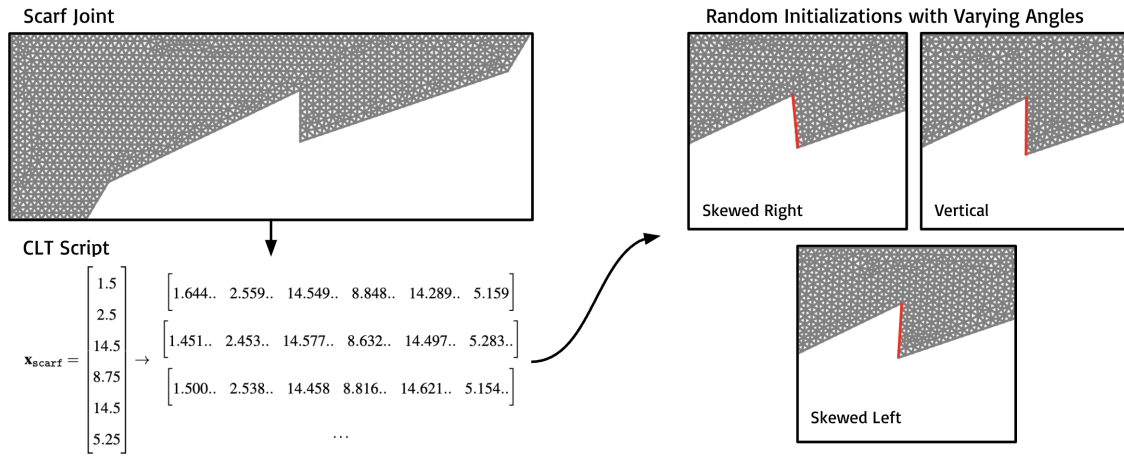


Figure 5: Randomized initializations of a scarf joint outputting varying angles to explore deeper local minima.

4.4. Optimization and 3D printing

This approach employs a built finite-element analysis gradient-descent method, where it utilizes an alternating penalty structure to optimize the interlocking joints' stiffness effectively. Systematically, it constrains one side of the joint as rigid while the other side deforms under a fixed load, which allows for the simulation of real-world mechanical stresses as shown in figure 6. The simulation tool adjusts for properly setting the contact between the given meshes and alternates until it provides an accurate tool to calculate the deformation measurements such as stress, strain, and displacement. From this, we can solve a constrained PDE that has been formulated for a system where a joint set by its DoF as parameters, is applied to a constraint such as the fixed load and thus reduces the amount of displacement. The adjoint method is utilized to solve this as it sets up the gradient of a

constrained PDE towards its parameters and allows for this minimization. Likewise, it is set such that the minimization of the displacement in turn maximizes the stiffness of a joint, and this process converges after 15 iterative gradient descent steps for one set of parameters in the tool provided [9]. However, given that this approach uses a random initialization tool, there are over 20 different sets of parameters for a given joint configuration, and would require over 2-3 hours of compute time to achieve the optimized parameters \mathbf{o} .

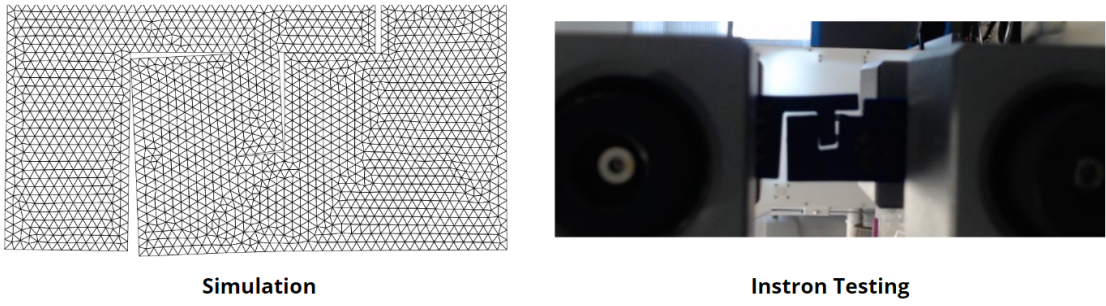


Figure 6: Comparison of the FEM simulation with a real life tensile test at 80N with the Instron.

Additionally, to test the optimized parameters, an empirical evaluation must be conducted using an Instron universal testing machine. Universal testing machines allow for the setup of a tensile test; which inherently measures the mechanical properties of materials under tension by pulling apart the joints, allowing for the calculation of stiffness. This tool also provides precise control over the load application, ensuring that each joint undergoes the same conditions for accurate comparisons needed. As the optimization provides 20 different sets of optimized parameters, for evaluation purposes with the Instron, we can choose the top-k joints with minimized displacements, as they provide the maximum stiffness parameters for a configuration. Initially, the top 2 joints were going to be selected for evaluation but given the allotted time restrictions and availability of machines, our approach would choose the best joint parameters as the top 2 had relatively similar performance and parameters across all shape configurations. For each set of joint parameters, both initial \mathbf{x} , and optimized \mathbf{o} , three prototypes are produced using 3D printing. This replication ensures that the test results account for any variability in the printing process which ensures a robust dataset for evaluation.

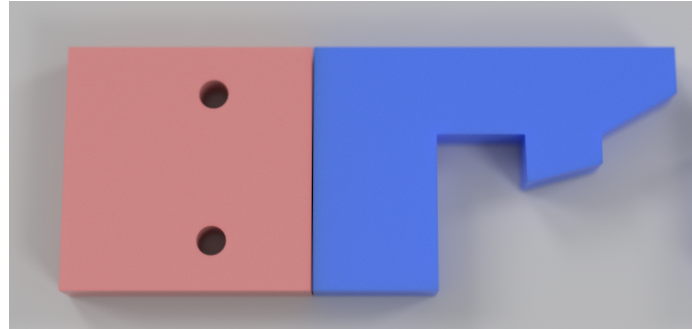
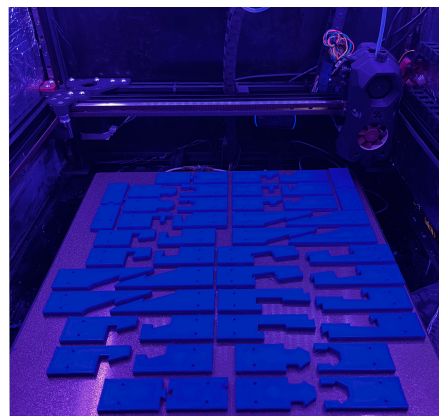


Figure 7: 25 × 25mm clamp space shown with the red section of the Optimized Lap Joint.

As for the 3D printing, Autodesk Fusion was required to accurately draw the joints with the joint parameters. We meticulously adjusted the designs to include a 0.2mm gap between joint components to account for the expansion of filament, thus making the joints easily assemblable. Additionally, each design consisted of a 25mm by 25mm clamp space equipped with 3mm mounting holes shown in figure 7, allowing for an adjustable clamping space to fit the grippers of the Instron machine as needed. Utilizing Prusa Slicer, the models were configured with a gyroid pattern at 20% density, 0.2mm layer thickness, three layered walls with five solid top and bottom layers to balance the use of the PETG material and give the joints structural integrity under the fixed load. We used a Voron 2.4 350mm printer, with serial number V2.3723, which had been precisely calibrated before each print to ensure minimal warping. A total of 36 joints were required for the evaluation, and we printed two sets of 24 joints to ensure an adequate sample size as shown in figure 8. This rigorous setup allowed for us to produce joints under consistent conditions which allows for our reliable testing.

Figure 8: 24 joints 3D printed using the Voron 350mm printer.



5. Evaluation

In this section, we will discuss the systematic process of evaluating the optimized designs of the various interlocking joints concerning their stiffness. This assessment is designed to evaluate across 36 interlocking joints conducted with an Instron machine, model 34SC-5 and equipped with grippers 2710-155. These were specifically chosen for their precision and compatibility with the types of joints being tested. We subject each joint to a variable 500N load and prematurely stopping at 80N. This allows for the detailed analysis of the forces within the joints under stress. Moreover, this procedure not only verifies the effectiveness of the optimization technique as we compare it to the initial attempts, but it also provides valuable information on the robustness and durability of the joints. Through this rigorous protocol, we aim to demonstrate the practical evaluation of joint performance due to the gradient-based optimization and our tailored approach to various joints.

5.1. Experiment Setup

For the experimental setup, we meticulously prepared each joint to ensure that we had a uniform procedure. Before testing, the joints were labeled with their respective dimensions, labeled as either initial or optimization versions, and provided a number to match their corresponding printed part. Now to ensure that we provided the same distribution of load to the joints, a horizontal line was drawn at the 25mm mark from the ends of each side of the joint. The labeled joints can be seen in figure 9, where we have a total of 48 joints, but as we have some joints that have slightly warped we've limited our testing space to 36. Moreover, this procedure didn't require us to mount an additional clamping space as the grippers provided a precise fit to the respective joint thickness.

Notably, we utilized the Bluehill Universal software provided by the Instron machine to create a testing method that was set with the necessary criteria to evaluate the joints. Within the software, we provided the respective dimensions of each sample and labeled them to distinguish between initialized and optimized joints to provide meaningful data. In terms of evaluation criteria, we specifically relied on analyzing performance relative to stiffness which is calculated as load per displacement (F/mm). In terms of calculating these metrics, we follow a similar methodology from

Sun's research, where we evaluate the stiffness of each joint at 30N and 60N intervals to detect performance differences across the joints under these specified loads. To ensure that we deter any abnormal loads, we start Instron at 0N of load and set it to progress at a rate of 20mm per minute. We enable the end-of-test criteria where we set an upper force limit at 80N to prevent damage to the joints and maintain a precise force application within the range. Ultimately, we provide a high-quality camera to record the progress and export a CSV containing our provided metrics and include stress and strain for future analysis.



Figure 9: Labeled and Organized Joints

Correspondingly, we must provide a robust procedure to allow the machine to follow this method. We begin by setting one side of the joint to the fixed bottom gripper at the marked line, keeping it level and firmly clamped. The following joint side is attached and the top gripper is lowered until the marked line, we move the inner clamps until it is a leveled setup. After clearing the workspace, the Instron machine is unlocked and the tensile test is performed. After it meets the 80N threshold, the joint gets removed by unclasping one side of the machine, this allows for a repeated process against the other samples. For every joint, including a baseline dovetail joint, the procedure is repeated across 6 samples, split by initial and optimized versions, and recorded their stiffness. These values are split based on their label, averaged accordingly, and then formatted such that we include a \pm of one standard deviation to ensure that our metrics provide certain measurements as shown below. Let s_i represent the stiffness measurement for sample i , where $i \in 1, 2, \dots, 6$ and init and

`opt` are labels that subset the samples, i.e. S_{init} .

$$\text{For label init: } \mu_{\text{init}} = \frac{1}{|S_{\text{init}}|} \sum_{i \in S_{\text{init}}} s_i, \quad \sigma_{\text{init}} = \sqrt{\frac{1}{|S_{\text{init}}|-1} \sum_{i \in S_{\text{init}}} (s_i - \mu_{\text{init}})^2}$$

$$\text{Stiffness for label init: } \mu_{\text{init}} \pm \sigma_{\text{init}}$$

To give an overall average percentage of stiffness gained/loss we can evaluate these models with the following:

$$\frac{\mu_{\text{opt}} - \mu_{\text{init}}}{\mu_{\text{init}}} * 100$$

5.2. Results

Given that we evaluated 36 samples, the following subsection will be divided up in terms of similar trends and respective performance.

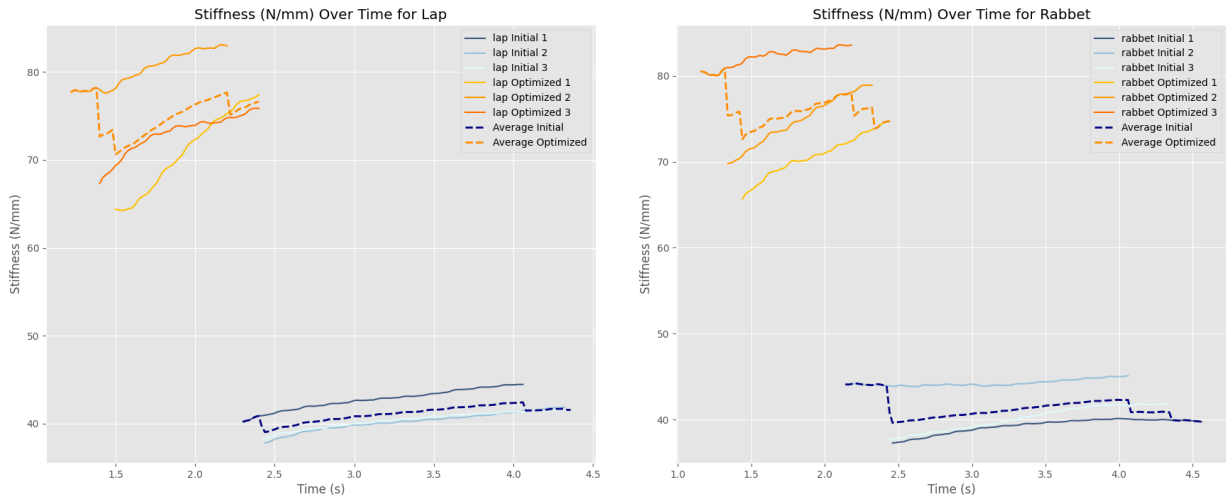


Figure 10: Stiffness vs. Time for Lap and Rabbet Joints

The plots shown in figure 10, represent the change in stiffness over time relative to the 30-60N range of force applied. The sample sets are divided on their initial and optimized labels, where in the case of lap and rabbet joints, there are key insights in their improvement. Within both sets of the initialized version, we see a plateau in the stiffness-time curve, whereas the optimized versions are significantly higher and increasing. However, after evaluating the structure of the curves, they

closely resemble a logistic function. The stiffness plateaus around 1.5 to 2.5 seconds, meaning there isn't much room for improvement and thus keeping the load position change within 30N to 60N provides an adequate space for evaluation. Performance is rated around 80 percent for both joints across their evaluations as shown in table 2. Furthermore, the low variability in our results provides a strong basis to assert that the FEM optimization technique significantly enhanced performance.

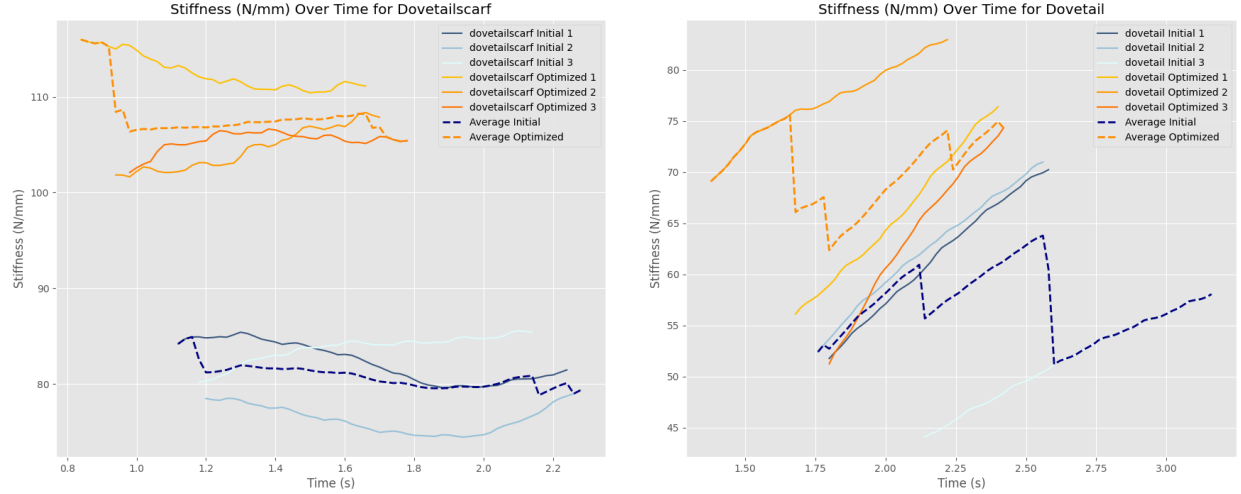


Figure 11: Stiffness vs. Time for Dovetail and Dovetail-Scarf Joints

For our dovetail-scarf joint, both initialized and optimized joints have a relatively plateau slope, but overall we can see a decent improvement in the given stiffness of the joints. The performance relative to the two previous isn't as significant in terms of the P-30 and P-60 percentages presented in table 2, but it has the second highest stiffness with a peak of 108.10 N/mm in the OS-60 evaluation. Now in terms of the dovetail joint, it had the least positive performance across these joints, and it could confide in the initialized attempt already being a near-optimal solution. Rerunning the parameters with the randomized initialization could have possibly explored steeper gradient descents, in which the joint width had become smaller and gave an aggressive angle. These improvements could be seen within figure 11, where the curves are relatively close. Despite this, it provides significant insights into the random initialization tool exploring better local minima and aiding the optimization technique.

Lastly, we take a look at the last two joints which have some contradictory performances

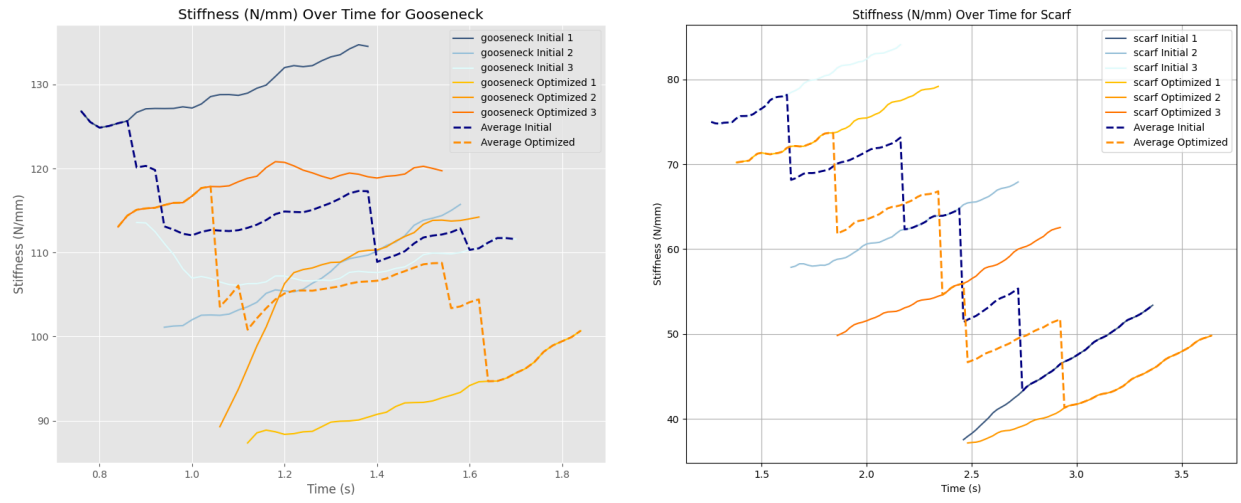


Figure 12: Stiffness vs. Time for Gooseneck and Scarf Joints

considering the improvements shown before. Overall, we see that the initial IS-60 categories provide the highest stiffness across the two joints signifying that the optimization technique suffered when applying these two joints. However, there is a significant difference in the variance of the stiffness whereas the other scenarios had relatively small deviations and provided concise results. Within the graphs of figure 12, there are many instances where the initialized and optimized curves overlap and alternate.

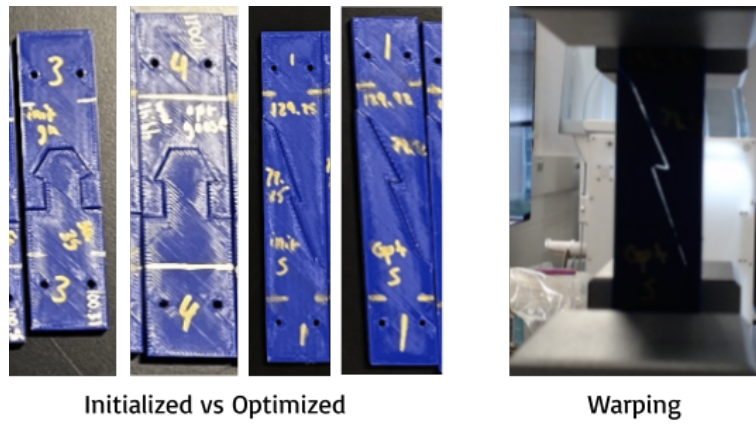


Figure 13: Similar design parameters but angle changes after optimization, and warping in the 3D prints provided a gap that introduced vulnerabilities.

| Joint | IS-30 ($\frac{N}{mm}$) | OS-30 ($\frac{N}{mm}$) | IS-60 ($\frac{N}{mm}$) | OS-60 ($\frac{N}{mm}$) | P-30 (%) | P-60 (%) |
|-----------|--------------------------|--------------------------|--------------------------|--------------------------|----------|----------|
| Lap | 38.70 ± 1.04 | 69.56 ± 5.67 | 42.64 ± 1.29 | 78.70 ± 2.99 | 79.77 | 84.57 |
| Rabbit | 39.71 ± 3.13 | 71.78 ± 6.47 | 42.19 ± 2.25 | 79.10 ± 3.62 | 80.77 | 87.49 |
| Dovetail | 49.24 ± 3.79 | 58.38 ± 7.38 | 66.63 ± 5.94 | 78.13 ± 3.48 | 18.57 | 17.26 |
| DoveScarf | 80.850 ± 2.233 | 106.60 ± 6.79 | 82.18 ± 2.35 | 108.10 ± 2.33 | 31.85 | 31.54 |
| Scarf | 56.79 ± 15.45 | 52.35 ± 13.62 | 68.73 ± 12.51 | 63.93 ± 12.04 | -7.82 | -6.982 |
| Gooseneck | 114.04 ± 10.76 | 96.28 ± 11.77 | 120.73 ± 9.89 | 111.73 ± 7.67 | -15.57 | -7.46 |

Table 2: Overall stiffness dataset across the various joints, IS and OS representing initialized and optimized stiffness. These are distinguished by 30N and 60N intervals, and the performance is represented in our P-30 and P-60 columns. The bold numbers represent the highest stiffness average for a particular joint.

These variances could signify that the initialized versions were already optimal solutions or that the test subjects weren't properly leveled during these steps. However, when taking a closer look at the shape designs, most of the parameters didn't relatively change except the angle of the contacting edges where they conform into a more horizontal position as shown in figure 13. These design changes perform a similar pattern to the dovetail joint implementation where the angle had slightly changed and provided a better local minimum. Therefore, taking a deeper look into the recordings, there was a clear indication that both of these joints had some warping in the prints causing them to form a significant gap. This provides a strong basis for the high variance within the logistic curves, and thus requires us to ensure proper prints and take future looks into hyper-tuning methods to enhance the technique.

6. Conclusion

Drawing upon these evaluations, there is a clear indication that this project achieved considerable success in most instances. Provided with the FEM optimization technique, we had significant improvements in the stiffness metrics, in particular with the lap and rabbet joints, which saw performance enhancements around 80 percent. This notable performance not only aligns with the core objectives of the project but also emphasizes the resourcefulness of using gradient-descent to solve PDEs. Analogously, we saw a clear indication of improvements concerning using randomized initialization shown in the dovetail joint as it provided slight improvements.

Despite these improvements, we did note some cases where from a first glance, the optimization technique did not perform well. However, it is quick to note that the scarf and gooseneck joints could've been optimal solutions to the PDE as seen with the dovetail joint. Therefore they could've provided higher improvements if it weren't for the noticeable warping in the joints that had made a significant gap when the Instron performed the tensile experiments. These deviations provide valuable insights into refining our process to account for nuances such as print quality and material behavior, and we anticipate further improvements by fine-tuning the hyperparameters to enhance the robustness.

Overall, our ambition was not only to maximize the stiffness of various interlocking joints but also to broaden the use of intricate interlocking joints to reduce the need for adhesives and metal fasteners. These improvements provide a basis for contributing to sustainability and cost-effectiveness in the manufacturing scene. The positive outcomes observed signify a step forward in this endeavor, and not only has it advanced our understanding of joint optimization but it lays the foundation for applying this to even more diverse sets of interlocking joints.

7. Future Work

7.1. Hyperparameter Tuning

Given our results, hyperparameter tuning would provide a promising avenue for further refinement of the FEM optimization technique. Systematically adjusting parameters would allow for fine-tuning our models to achieve higher performance. Future developments of this technique can explore a range of methods such as grid search to navigate the complex optimization domain. Likewise, an application of Bayesian optimization provides an automatic approach that can optimize the performance of a learning algorithm for their model hyperparameters [8]. Through these efforts, we can further extend to the fields of sustainable designs and advanced manufacturing.

7.2. Amortized Implementations

Building upon our choice of optimization technique, the simulations required about 1.5-2 hours to converge with randomized initialization. Future developments can explore alternative methodologies to solve the PDE more efficiently. Specifically, there are other advanced techniques such as stochastic gradient descent, momentum-based gradient descent, and physics-informed neural networks (PINNs) [7], [2]. These methods address some limitations observed with the vanilla gradient descent approach, such as slow convergence rates and entrapment in local minima. By experimenting with these variants and comparing their performance, we can identify more efficient and more globalized optimization outcomes to enhance the development of these joints.

8. Acknowledgements

I would like to thank my advisor, Professor Ryan Adams for his invaluable insights and guidance throughout this semester. Likewise, I extend my gratitude to our teaching assistant, Aditya Palaparthi, for his support and adeptness in addressing multiple questions with constructive insights. I would also like to thank Xingyuan Sun, for providing the base implementation of the finite simulation software. In regards to the 3D portion of this paper, I would like to thank David Bershadsky ECE '24 for lending his printer, and Ernesto Moreno COS '25 for their indispensable guidance on CAD work. Finally, I extend my gratitude to CEE Ph.D. Candidate, Isabel M. de Oliveira, for allowing me to use the Instron Machine needed for evaluation and her clever insights regarding material sciences.

References

- [1] J. S. Dokken *et al.*, “Shape optimization using the finite element method on multiple meshes,” *arXiv*, Jun. 2018. Available: <https://arxiv.org/abs/1806.09821v1>
- [2] T. G. Grossmann *et al.*, “Can physics-informed neural networks beat the finite element method?” *arXiv*, Feb. 2023, available: arXiv.org. Available: <https://arxiv.org/abs/2302.04107>
- [3] Y. Hahn and J. Cofer, “Design study of dovetail geometries of turbine blades using abaqus and insight,” vol. 7, 06 2012.
- [4] M. Larsson *et al.*, “Tsugite: Interactive design and fabrication of wood joints,” in *ACM Conferences*. University of Tokyo, Oct. 2020. Available: <https://dl.acm.org/doi/10.1145/3379337.3415899>
- [5] S. McNulty-Kowal, “A japanese joinery method integrated in these reusable pencils helps utilise those tiny pencil stubs,” Yanko Design - Modern Industrial Design News, Feb. 2022. Available: <https://www.yankodesign.com/2022/02/26/a-japanese-joinery-method-integrated-in-these-reusable-pencils-helps-utilise-those-tiny-pencil-stubs/>

- [6] M. N. Nguyen *et al.*, “Corrosion effects in the structural design of metal fasteners for timber construction,” *Structure and Infrastructure Engineering*, vol. 9, no. 3, pp. 275–284, 2013. Available: <https://doi.org/10.1080/15732479.2010.546416>
- [7] S. Ruder, “An overview of gradient descent optimization algorithms,” *arXiv*, Jun. 2017, available: arXiv.org. Available: <https://arxiv.org/abs/1609.04747>
- [8] J. Snoek, H. Larochelle, and R. P. Adams, “Practical bayesian optimization of machine learning algorithms,” *arXiv*, Aug. 2012, available: arXiv.org. Available: <https://doi.org/10.48550/arXiv.1206.2944>
- [9] X. Sun *et al.*, “Gradient-based dovetail joint shape optimization for stiffness.” ACM: Proceedings of the 8th Annual ACM Symposium on Computational Fabrication, Oct. 2023, available: arXiv.org. Available: <https://doi.org/10.48550/arXiv.2310.19798>

9. Appendix

Complete code for the gradient-based optimization of interlocking joints using FEniCS is detailed in the GitHub repository, including execution instructions. Datasets for the initialized and optimized parameters, alongside evaluation metrics and videos of the experiments are provided as well.

<https://github.com/javierlinero/gradient-optimized-joints>